Physical, structural and mechanical characterization of $Ti_{1-x}Si_xN_y$ films

F. Vaz[a], L. Rebouta[a,*], S. Ramos[b], M.F. da Silva[c], J.C. Soares[d]

[a]*Dept. Física, Universidade do Minho, Campus de Azurém, 4810 Guimarães, Portugal*
[b]*ICMES—Fac. Ciências e Tecnologia da Universidade de Coimbra, 3030 Coimbra, Portugal*
[c]*ITN, Dept. de Física, E.N.10, 2685 Sacavém, Portugal*
[d]*CFNUL, Av. Prof. Gama Pinto, 2, 1700 Lisboa, Portugal*

Abstract

Within the frame of this work, $Ti_{1-x}Si_xN_y$ hard coatings with $0 \leq x \leq 0.37$ and thicknesses ranging from 1.2 to 3.5 μm, were prepared by r.f. reactive magnetron sputtering in an Ar/N_2 gas mixture. X-ray diffraction and Fourier analysis of X-ray profiles were used to investigate the structure and grain size, and its correlation with hardness behaviour, as a function of the Si content, bias voltage and working gas (argon) flow rate. In this respect, the results show that a double cubic phase of NaCl type was developed with lattice parameters of 4.18 and 4.30 Å, revealing the (111) orientation for low Si content ($x=0.05$), (220) for intermediate Si contents ($0.13 \leq x \leq 0.22$) and (200) for the highest Si contents ($0.30 \leq x \leq 0.37$). Regarding the results of ultramicrohardness tests, and although all samples with $0.05 \leq x \leq 0.30$ present a hardness value higher than 30 GPa, the $Ti_{0.85}Si_{0.15}N_{1.03}$ revealed the highest hardness value, around 47 GPa, which is more than twice as high as that of common TiN. Furthermore, the study of hardness as a function of the applied bias voltage revealed that best results are achieved between −50 and 0 V. The variation in hardness as a function of the argon flow showed that best results in hardness are obtained when working with flow rates around 110 cm^3/min. © 1998 Elsevier Science S.A. All rights reserved.

Keywords: Hard coatings; Titanium and silicon nitride; Grain size; Texture

1. Introduction

Surface engineering using applied coatings has become a well-established technology and it is an extremely versatile mean of improving component performance [1]. The increasing importance and use of these surface coatings brought an increasing need for fundamental understanding of their properties if the optimum coating for a particular purpose is to be selected. Furthermore, there is a general agreement in literature that the performance of tools and components in a tribological, corrosive or mechanical loaded environment is mainly determined by the properties of near-surface layers [2]. This implies that the solutions to achieve a coating tailored for a particular task will essentially depend on the ability to establish a knowledge of the interrelationship between their physical, structural and mechanical properties. In order to maintain or increase the lifetime of tools or any other tribological system, a broad variety of different hard coatings have been developed, tested and used in industry and a large

collection of results can be found in the literature [3–5]. Furthermore, new materials such as superhard diamond, cubic boron nitride and some based carbides and nitrides, offer prospects for the development of new technologies which are having a significant impact on everyday life. One of the most promising materials are the systems consisting of a nanocrystalline transition metal nitride/amorphous Si_3N_4 composites, nc-MenN/a-Si_3N_4, Me=Ti, W, V, which can reach a hardness of about 50 GPa [6–8].

The indentation testing to provide information about the mechanical properties of a particular coating is nowadays one of the easiest, simple, and suitable for micromechanical analysis, and it has thus been widely used. However, to obtain a 'true' hardness value for a film that is not influenced by the substrate, the area of the contact impression must be kept small relative to the film thickness. A comprehensive rule of thumb is that the depth of the contact should be less than 10% of the film thickness [9], though in some materials substrate independent measurements have been claimed for depths of up to 25% [10]. These restrictions are becoming more severe, especially in the case of a hard film on a soft substrate [11,12]. In either case, the hardness impressions for films with micron dimensions must be so small that their areas cannot be

*Corresponding author. Tel.: +351-53-510151; fax: +351-53-678981;
e-mail: Rebouta@fisica.uminho.pt

accurately determined by optical means. To overcome this restriction, a microindentation testing method with a load resolution of a few mN is now available, and its use is widely accepted. This method involves making a small indentation in the film, usually with a Berkovich or a Vickers indenter, while continuously recording the indentation load, L, and displacement, h, during one complete cycle of loading and unloading [13].

In this paper we have studied $Ti_{1-x}Si_xN_y$ coatings deposited on steel substrates and produced by reactive magnetron sputtering. These samples allowed studying the evolution of hardness for a range of different chemical compositions, substrate bias voltage and working gas flow. The hardness as a function of these parameters and its correlation with the developed texture and grain size will be analysed and discussed in some detail.

2. Experimental details

2.1. Sample materials

The $Ti_{1-x}Si_xN_y$ samples were deposited by reactive r.f. magnetron sputtering from high purity Ti and Si targets onto polished high-speed steel (AISI M2) and silicon substrates. The depositions were carried out in an Ar/N_2 atmosphere in an Alcatel SCM650 apparatus. All substrates were sputter etched for 15 min in a pure Ar atmosphere with a 200 W r.f. power. The target to substrate distance was kept at 60 mm in all runs and the substrate holder was rotating over the targets at a constant speed of 4 rpm. The base pressure in the deposition chamber was about 10^{-4} Pa and rose to values around 4×10^{-1} Pa during depositions. The substrates were heated to 300°C and d.c. biased from -75 up to 25 V. The experiments were carried out with the titanium and silicon targets coupled to r.f. sources (13.56 MHz), with powers in the range of $1.9–3.2 \times 10^4$ W m^{-2} for Ti and $0.8–2.6 \times 10^4$ W m^{-2} for Si. The atomic composition of the as-deposited samples was measured by Rutherford backscattering spectrometry (RBS). An average number of five 'ball cratering' (BC) experiments were carried out in each sample in order to determine its thickness. X-ray diffraction (XRD) experiments were undertaken in a Philips PW 1710 apparatus using a Cu Kα radiation, in order to obtain texture. Also, sample grain size evaluation was conducted from Fourier analysis of X-ray diffraction line profiles. Since in our samples only one first-order diffraction profile is usually available, the method introduced by Mignot and Rondot [14] was used, which is based on the analysis of a single X-ray profile. This method uses a hyperbolic law to describe the microstrain term, $\bar{\epsilon}_n^2 = C/n$, in which, n is the harmonic number of the Fourier coefficients. A two-degree polynomial is then fitted to the Fourier coefficients, which polynomial parameters give the grain size.

2.2. Hardness and Young's modulus measurement technique

2.2.1. Instrumental set-up

The ultramicrohardness tests were performed in a computer-controlled Fischerscope H100 ultramicrohardness tester, equipped with a quadrangular pyramidal Vickers diamond indenter. The applied load was increased in 60 steps until the nominal load reached 30 mN, which was the maximum load in all tests. The same steps were used for the unloading stage. The system has a load resolution better than 1 μN and the range of the nominal test load is between 4 mN and 1 N. At the beginning of each test, the indenter approached the sample at a rate of 1 μm/s and the indentation depths are obtained with a capacitance displacement gage accuracy of 2 nm. An average number of 15 tests were performed in each sample. For samples where some dispersion occurred, 10 additional tests were performed.

2.2.2. Hardness and Young's modulus evaluation

The key quantities to obtain a ultramicrohardness value are the peak load, P_{max}, the displacement at peak load, h_{max}, the initial unloading contact stiffness, $S = dP/dh$, which represents the slope of the initial portion of the unloading curve and the displacement, which is found by linearly extrapolating the initial portion of the unloading curve to zero load [13], h_p.

The hardness, calculated as the ratio of the applied load, P_{max}, to the projected area, A, of the contact between the indenter and the test piece, can be directly related to h_p by [15]:

$$H_v = \frac{P_{max}}{A} = \frac{P_{max}}{C \cdot h_p^2} \tag{1}$$

where C is the ratio of the projected area A to the square of the penetration depth h_p (which is a constant for a given indenter, e.g. $C = 24.5$ for a four-sided Vickers indenter [13]).

The Young's modulus, E, can be calculated by the slope of the initial portion of the unloading curve by adopting Sneddon's flat-ended cylinder punch model [16]. By equating the projected area, A, to the punch area and putting the equation in the form of unloading slope, one has:

$$S^{-1} = \frac{dh}{dP} \cdot \frac{1}{2} \cdot h_p \cdot \left(\frac{\pi}{24.5}\right)^{1/2} \cdot \left(\frac{1}{E_r}\right) \tag{2}$$

where $1/E_r = (1 - \nu_f^2)/E_f + (1 - \nu^2)/E_i$, with E_f and ν_f being the Young's modulus and Poisson's ratio for the film ($\nu_f = 0.25$) [17] and E_i and ν_i, the same quantities for the diamond indenter ($E_i = 1141$ GPa and $\nu_i = 0.07$ [18]).

2.2.3. Experimental corrections

In order to achieve reasonable accurate values of hardness, the instrument shall be traceably calibrated with respect to load, displacement, instrument frame stiffness and indenter area function. In the equipment used for this work, two main corrections were taken in consideration:

2.2.3.1. Calibration of the thermal drift

This correction appears as a need to overcome the drift in displacement due to mechanical vibration and/or temperature fluctuations. In the case of ultramicro- and nanohardness measurements, this correction becomes very important, being responsible for an important decrease in hardness values, which may be reduced in more than 1000 Vickers in some cases. In our experiments, this correction was obtained by linear fitting of the hold period (30 s) at final unloading stage (0.4 mN).

$$h_{ptd} = h_p \cdot corr \cdot t \tag{3}$$

where the term corr represents the slope of that linear fitting and t the time interval correspondent to each point.

2.2.3.2. Calibration of the indenter offset

This correction is the result of some geometrical imperfections of the indenter—the so-called tip offset [19]. This tip offset is specific for each apparatus and is usually responsible for higher hardness values, especially for very small indentation depths such as the ones used in this work. For our equipment, and due to this factor, the thermal drift corrected indentation depth, h_{ptd}, is then corrected by the expression [19]:

$$h_{pc} = 0.052 + 1.095 \cdot h_{ptd} \tag{4}$$

The term h_{pc} represents the final corrected indention depth value.

3. Results and discussion

3.1. Characterisation of the as-deposited samples

The analysis of the $Ti_{1-x}Si_xN_y$ samples was carried out in three distinct groups. The first one includes the samples grown with the same bias voltage (-50 V), but with different Ti/Si target power combinations. The second group deals with the samples produced with the same deposition parameters, except the different applied bias voltage, which varied from -75 to $+25$ V. For this group, the composition of the different samples was approximately constant, $Ti_{0.83}Si_{0.17}N_{1.06}$, although a small increase in the Si content was observed for the positive biased samples ($x=0.22$ and $x=0.20$ for 15 and 25 V, respectively). Finally, a third group, which is a result of a set of experiments where the only deposition parameter that has varied was the argon flow rate. In these experiments the argon flow rate varied from 60 to 180 cm^3/min and the observed composition was about $x=0.34$ except for the sample prepared with an argon flow of 110 cm^3/min, which has $x=0.29$. Table 1 presents a summary of deposited coatings (first group), together with the thickness measurements (BC), grain sizes (XRD) and the atomic composition (RBS). As an example, Fig. 1 shows X-ray diffraction patterns obtained from the as-deposited samples as a function of the applied bias voltage. These results reveal the presence of two different crystallographic structures, both indexed to the cubic structure and with lattice parameters of about 4.30 Å (phase 1) and 4.18 Å (phase 2).

Starting with the samples with different Ti to Si contents (same bias and argon flow), three distinct situations were observed. For the samples with the lowest Si content ($x=0.05$) a (111) preferred growth orientation was obtained with a grain size of about 8 nm, which is very similar to what we have obtained for our TiN samples, deposited also in rotation mode. The samples with intermediate Si content ($x=0.12$, 0.15, 0.17 and 0.22) revealed a (220) preferential growth orientation. Fourier analysis of X-ray diffraction line profiles, yield grain sizes of about 7 nm in the first and third ones and 6 nm for the other two samples. Finally, the samples with the highest Si content ($x=0.30$ and 0.37) developed a grain growth essentially on the (200) direction and grain sizes between 5 and 6 nm.

Regarding the variation in bias voltage, some interesting changes were induced in the relative fraction of each phase. Regarding the samples deposited with positive bias values (0, 15 and 25 V), only phase 2 with the (111)

Table 1
Thickness, composition and grain size of the samples

Coating	Ti (at%)	Si (at%)	N (at%)	Ar flow (cm^3/min)	Bias (V)	Thickness (μm)	Grain size (nm)
TiN	50	—	50	100	-50	3.3	7
$Ti_{0.95}Si_{0.05}N_{1.02}$	47	2.5	50.5	100	-50	1.6	8
$Ti_{0.88}Si_{0.12}N_{1.04}$	43.1	5.9	51	100	-50	2.2	7
$Ti_{0.85}Si_{0.15}N_{1.03}$	41.9	7.4	50.7	100	-50	2.1	6
$Ti_{0.83}Si_{0.17}N_{1.06}$	40.3	8.3	51.4	100	-50	1.3	7
$Ti_{0.78}Si_{0.22}N_{1.07}$	37.7	10.6	51.7	100	-50	2.2	6
$Ti_{0.70}Si_{0.30}N_{1.10}$	33.3	14.3	52.4	100	-50	2.2	5
$Ti_{0.63}Si_{0.37}N_{1.12}$	29.7	17.5	52.8	100	-50	3.2	6

The error in the N atomic composition is about 3 at%. All samples, except $Ti_{0.70}Si_{0.30}N_{1.10}$, were produced with a 350-nm thick Ti adhesion layer.

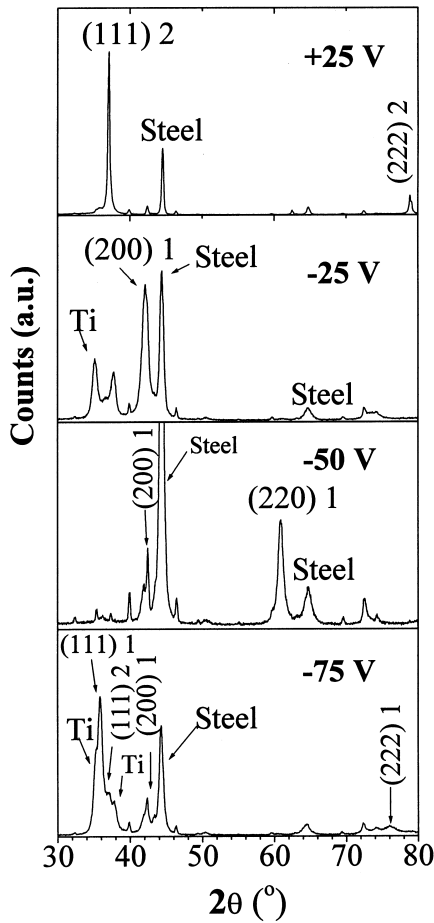Fig. 1. X-ray diffraction patterns of $Ti_{1-x}Si_xN_y$ films deposited with bias voltage in the range −75 to +25 V.
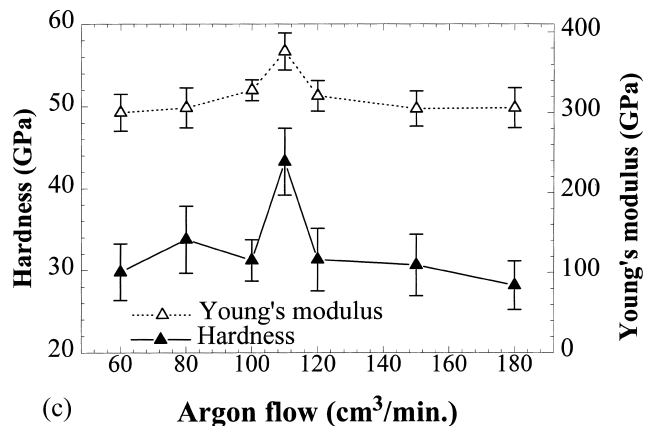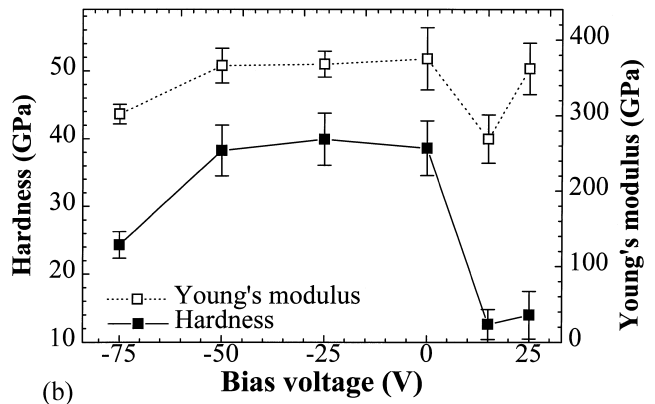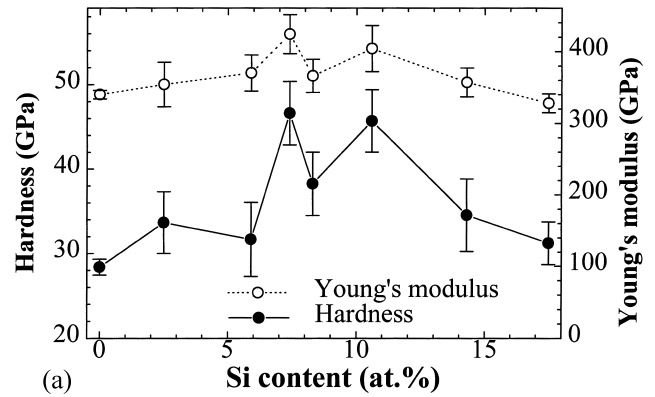

Fig. 2. Ultramicrohardness values and Young's modulus of $Ti_{1-x}Si_xN_y$ samples as a function of the Si content (a), bias voltage (b) or argon flow (c).

preferred orientation was observed, revealing relatively large grains (23, 25 and 34 nm, respectively). On the other hand, for the samples deposited with negative bias voltage, two distinct situations have been identified. The one prepared under −25 V developed a (200) preferred orientation and a very small grain size (around 7 nm). The −50 V one grows essentially on the (220) direction, revealing a grain size of about 5 nm. Both samples are indexed with phase 1. For a bias voltage of −75 V, a mixture of the two phases was observed, being phase 2 with a (111) preferred orientation and phase 1 with a mixture of (111) and (200) orientations and grain sizes of about 5.5 nm.

Finally the results as a function of the argon flow revealed that all samples grew on the (200) orientation of phase 1, except the one prepared with 180 cm³/min, which also shows that two phases mixture.

3.2. Characterisation of ultramicrohardness

From the observation of Fig. 2a, one can infer that for the $Ti_{1-x}Si_xN_y$ system, higher hardness values were ob-

tained for $Ti_{0.85}Si_{0.15}N_{1.03}$ (≈ 47 GPa). Although the $Ti_{0.63}Si_{0.37}N_{1.12}$ showed a very small grain size, its hardness value is very low (even lower than that of TiN), which we believe it might be due to its relatively high Si content. However, this seems to be the apparent behaviour of the $Ti_{1-x}Si_xN_y$ system, which shows a significant increase in hardness until a maximum Si content of $x = 0.15$, decreasing then until values smaller than those obtained for TiN. A closer look to the X-ray diffraction patterns, shows that this behaviour can be closely corre-

lated to the obtained patterns. Hence, best results correspond to the (220) preferential grain growth, while those corresponding to (200) and (111) seem to indicate intermediate to lower hardness values. Not only the texture but also the grain size seems to be important for the improvement in hardness. The samples with $x = 0.12$, 0.15, 0.17 and 0.22, which grew on the (220) direction, are a particular example of this. The ones with the smallest grain size show exactly the highest hardness values.

Regarding the bias voltage (Fig. 2b), best results were obtained for the samples produced within the range −50 to 0 V and growing preferentially on the (220) and (200) orientation (phase 1) for the negative biased ones and (111) orientation (phase 2) for the one produced under no bias voltage. The sample produced with a bias voltage of −75 V presents a low hardness value, and a preferential growth revealing the presence of a mixture of the two phases. Since its grain size is relatively small (around 5.5 nm), one can infer that the texture definitely plays an important role for its behaviour. The samples produced under positive bias, which have developed a growing direction on the (111) plane related to phase 2, revealed poor hardness values, presenting large grains (>25 nm). The sample prepared with no applied bias voltage presents a relatively high hardness value (around 38 GPa), although it grew essentially in the same direction as those produced under positive bias voltage. We believe that this behaviour might be related to the relative Si content, as referred before. From these observations one can infer that beyond Si content and texture, the grain size is also determinant for the coating hardness behaviour.

The results as a function of the argon flow (Fig. 2c) revealed that best results are achieved when working with an argon flow of 110 cm^3/min. No significant changes were visible in texture which may explain the little variation observed in hardness values.

4. Conclusions

XRD results show that a double cubic phase of NaCl type was developed in the $Ti_{1-x}Si_xN_y$ system with lattice parameters of 4.18 and 4.30 Å.

From the ultramicrohardness results, it has been shown that the $Ti_{1-x}Si_xN_y$ system has high hardness values for Si contents in the range $0.15 \leq x \leq 0.22$. These samples revealed a (220) preferential grain growth, while those with high Si contents ($0.30 \leq x \leq 0.37$) developed a (200) texture and that with low Si content ($x = 0.05$), the (111) preferential orientation. These last revealed intermediate to lower hardness values, which seems to indicate that texture

plays an important role for the system behaviour. Furthermore, the grain size is also important since once related with (220) texture ($0.12 \leq x \leq 0.22$), the ones with the small grain show the highest hardness values.

The results as a function of the bias voltage show that best results are achieved when working in the range −50 to 0 V. These samples grew preferentially on the (220) and (200) orientation (phase 1) for the negative biased ones and (111) orientation (phase 2) for the one produced under no bias voltage. No significant changes are visible in the texture of the samples deposited as a function of the argon flow, which may explain the little variation observed in hardness values.

References

[1] M. Ohring, The Materials Science of Thin Films, Academic Press, San Diego, 1992, pp. 547–588.
[2] A. Mattews, Protective coatings and thin films: synthesis, characterization and applications, in: Y. Pauleau, P. Barnas, BOOK TITLE NEEDED, Kluwer, Dordrecht, 1996, pp. 1–12.
[3] D.S. Rickerby, P.J. Burnett, Thin Solid Films 157 (1988) 195.
[4] L.F. Senna, Surf. Coat. Technol. 94–95 (1997) 390–397.
[5] L.F. Pocdhet, P. Howard, S. Safaie, Surf. Coat. Technol. 94–95 (1997) 70–75.
[6] S. Veprek, S. Reiprich, Li Shizhi, Appl. Phys. Lett. 66 (1995) 2640.
[7] S. Veprek, S. Reiprich, Thin Solid Films 268 (1996) 64.
[8] S. Veprek, Surf. Coat. Technol. 97 (1997) 15–22.
[9] H. Bückle, in: J.W. Westbrook, H. Conrad (Eds.), The Science of Hardness Testing and Its Research Applications, American Society for Metals, OH, 1973, pp. 453–491.
[10] M.F. Doerner, D.S. Gardner, W.D. Nix, J. Mater. Res. 1 (1987) 845.
[11] Y. Sun, T. Bell, S. Zheng, Thin Solid Films 258 (1995) 198.
[12] X. Cai, H. Bangert, Thin Solid Films 264 (1995) 59.
[13] G.M. Pharr, W.C. Oliver, MRS Bull. 7 (1992) 28–33.
[14] J. Mignot, Rondot, Acta Metall. 23 (1975) 1321.
[15] M.F. Doerner, W.D. Nix, J. Mater. Res. 1(4) (1986) 601–609.
[16] I.N. Sneddon, Int. J. Eng. Sci. 3 (1965) 47–57.
[17] E. Török, A.J. Perry, L. Chollet, W.D. Sproul, Thin Solid Films 154 (1987) 37–43.
[18] G. Simmons, H. Wang, Single Crystal Elastic Constants and Calculated Aggregate Properties: A Handbook, 2nd ed., MIT Press, Cambridge, MA, 1971.
[19] A.C. Trindade, A. Cavaleiro, J.V. Fernandes, J. Testing Evaluation 22(4) (1994) 365.